REVIEW

Ratcheting up protein translocation with anthrax toxin

Geoffrey K. Feld,[1] Michael J. Brown,[2] and Bryan A. Krantz[1,2,3]*

[1]Department of Chemistry, University of California, Berkeley, California 94720
[2]Department of Molecular and Cell Biology, University of California, Berkeley, California 94720
[3]California Institute for Quantitative Biosciences, University of California, Berkeley, California 94720

Received 24 January 2012; Revised 21 February 2012; Accepted 22 February 2012
DOI: 10.1002/pro.2052
Published online 28 February 2012 proteinscience.org

Abstract: Energy-consuming nanomachines catalyze the directed movement of biopolymers in the cell. They are found both dissolved in the aqueous cytosol as well as embedded in lipid bilayers. Inquiries into the molecular mechanism of nanomachine-catalyzed biopolymer transport have revealed that these machines are equipped with molecular parts, including adjustable clamps, levers, and adaptors, which interact favorably with substrate polypeptides. Biological nanomachines that catalyze protein transport, known as translocases, often require that their substrate proteins unfold before translocation. An unstructured protein chain is likely entropically challenging to bind, push, or pull in a directional manner, especially in a way that produces an unfolding force. A number of ingenious solutions to this problem are now evident in the anthrax toxin system, a model used to study protein translocation. Here we highlight molecular ratchets and current research on anthrax toxin translocation. A picture is emerging of proton-gradient-driven anthrax toxin translocation, and its associated ratchet mechanism likely applies broadly to other systems. We suggest a cyclical thermodynamic order-to-disorder mechanism (akin to a heat-engine cycle) is central to underlying protein translocation: peptide substrates nonspecifically bind to molecular clamps, which possess adjustable affinities; polypeptide substrates compress into helical structures; these clamps undergo proton-gated switching; and the substrate subsequently expands regaining its unfolded state conformational entropy upon translocation.

Keywords: protein translocation; protein unfolding; Brownian ratchet; nonspecific binding; proton motive force

Introduction

Proteins, organelles, metabolites, and various cargos are continuously transported into, out of, and around cellular compartments. Generally, these movements are catalyzed by macromolecular machines, which consume energy and directionally translocate along specific polymeric tracks. These polymer tracks come in various forms, including microtubules, nucleic acids, and polypeptides. While it is consistently observed that chemical energy is consumed to do mechanical work, the underlying molecular mechanisms of energy transduction and directed movement at the nanoscale level are poorly understood and remain intense areas of research.[1-7]

Biological processes occur on the nanoscale under ambient chemical and temperature conditions.

*Correspondence to: Bryan A. Krantz, Departments of Chemistry and of Molecular and Cell Biology, University of California, 476 Stanley Hall 3220, Berkeley, CA 94720.
E-mail: bakrantz@berkeley.edu.

Grant sponsor: NIH; Grant number: R01-AI077703.

Scientists have long mused about the ability of nanoscopic power devices to harness energy from their environments. The most famous thermodynamic trick of the 19th century is credited to Maxwell, who proposed in *Theory of Heat* how energy is statistically distributed in a population of gas molecules.[8] When Maxwell began to imagine the molecular world, he expressed a most remarkable "contradiction" by the conclusion of his manuscript, which he subtitled, "Limitation of the Second Law of Thermodynamics." To illustrate, he proposed a *Gedankenexperiment* (thought experiment) [Fig. 1(A)] involving a vessel divided into two sections, A and B. Each side contains a similar proportion of gas molecules with a similar distribution of velocities and temperature. The division between the two sections contains a hole with a trap door operated by a "being" who only permits the movement of the faster molecules from A to B, and concurrently the movement of slower molecules from B to A. The being, coined "Maxwell's demon" by Lord Kelvin[9] would "thus, without expenditure of work, raise the temperature of B and lower that of A, in contradiction to the Second Law of Thermodynamics."[8] Later, it was reasoned that because the demon would need precise information on each gas molecule to sort them by velocity, the entropy change of the system and surroundings upon creating a thermal gradient would not be less than zero. Obtaining and consuming that information came at a price, and Maxwell's *Gedankenexperiment*, in fact, obeyed the Second Law of Thermodynamics. The device is, therefore, an information-powered heat pump.

The drinking bird novelty device [Fig. 1(B)] patented by Sullivan in 1946 is now a famous staple demonstration in science classrooms all over the world.[10] Deliberately flirting with one's disbelief in perpetual-motion machines, the happy-go-lucky device teeters relentlessly, dipping its beak into a glass of water. At first glance, one may think the bird is a "free" energy device. Of course, there is a man behind the curtain: the drinking bird, like a Stirling heat engine, functions by means of a *required* thermal gradient (ΔT). [Evaporative cooling on the wetted bird beak creates the ΔT; see Fig. 1(B) for details.] As noted by Carnot, "the motive power undoubtedly increases with difference in temperature between the warm and cold bodies."[11] Thus a nonzero ΔT is the *driving force* that powers the heat engine to produce spontaneous motion.

Nanomachines as Ratchets

Further adoption of Maxwell's demon led Smoluchowski[12] and later Feynman[13] to propose a nanoscale heat-engine device in related *Gedankenexperiments*. Imagine a system with two thermal reservoirs; across the two reservoirs is a drive shaft containing a pulley, a rope, and a weight. Gas molecules in the hotter reservoir transfer random thermal energy to large vanes, albeit the applied forces are random in direction. An anisotropic sawtooth-patterned ratchet wheel resides within the cooler reservoir. The ratchet wheel engages a pawl that effectively biases rotation of the wheel in one direction. Therefore, while Brownian motion of particles contained within the hotter reservoir pushes the vaned wheel randomly in either direction, the pawl-and-ratchet device in the colder reservoir rectifies these random fluctuations, biasing net motion in the allowed direction; and hence the pulley and rope turn, lifting the weight.

The ΔT energy gradient across the reservoirs is an essential feature of the ratcheting nanodevice.[13] If stochastic motion within the pawl in the colder reservoir were on the order of that on the hotter vaned-wheel reservoir (i.e., the condition of thermal equilibrium), then the system could not possibly do useful work, and the weight could not be lifted. Thus the Smoluchowski-Feynman ratchet is a nanomechanical heat engine (analogous to Sullivan's drinking bird). In addition to a nonzero thermal gradient, the machine operates on the principle that the mean displacement of random motion is on the order of the period, L, of the spatially periodic potential function during the time in which the barrier is switched to its minimized state [Fig. 2(A)]. A diode represents an analogous ratchet-like component for an electrical circuit. A four-diode bridge device can rectify an oscillating electrical current produced by a magnet displaced at random through a coil of wire; however, the diode bridge cannot use Nyquist noise (random *equilibrium* thermal fluctuations of electrons in the electrical circuit) to do work. Thus the pawl in Feynman's ratchet, the one-way valve in Smoluchowski's ratchet, and the demon-operated trap door in Maxwell's *Gedankenexperiment* can be thought of as mechanical diodes; however, each is only capable of using *nonequilibrium* energy fluctuations, energy gradients (e.g. ΔT), or stores of ordered information to do useful work.

We can simulate net motion in the Smoluchowski-Feynman ratchet using a spatially anisotropic potential but not an isotropic one [Fig. 2(A)]. Here we depict the ratchet wheel as a linearized repeating anisotropic potential and the pawl as a movable particle. To keep the model simple, the pawl (particle) can move relative to a stationary ratchet wheel in effect. When the potential is momentarily *flashed off*, the ratchet particle can freely diffuse. In principle, these energy barriers can be modulated *on* or *off* by any number of means, as long as the barriers are approximately k_BT, when switched *off*. (T is the temperature, and k_B is the Boltzmann constant.) When the energy well is offset and anisotropic, the particle is more likely to cross a closer peak, rather than a more distant peak. When the potential is *flashed on*, the particle will have a significantly higher

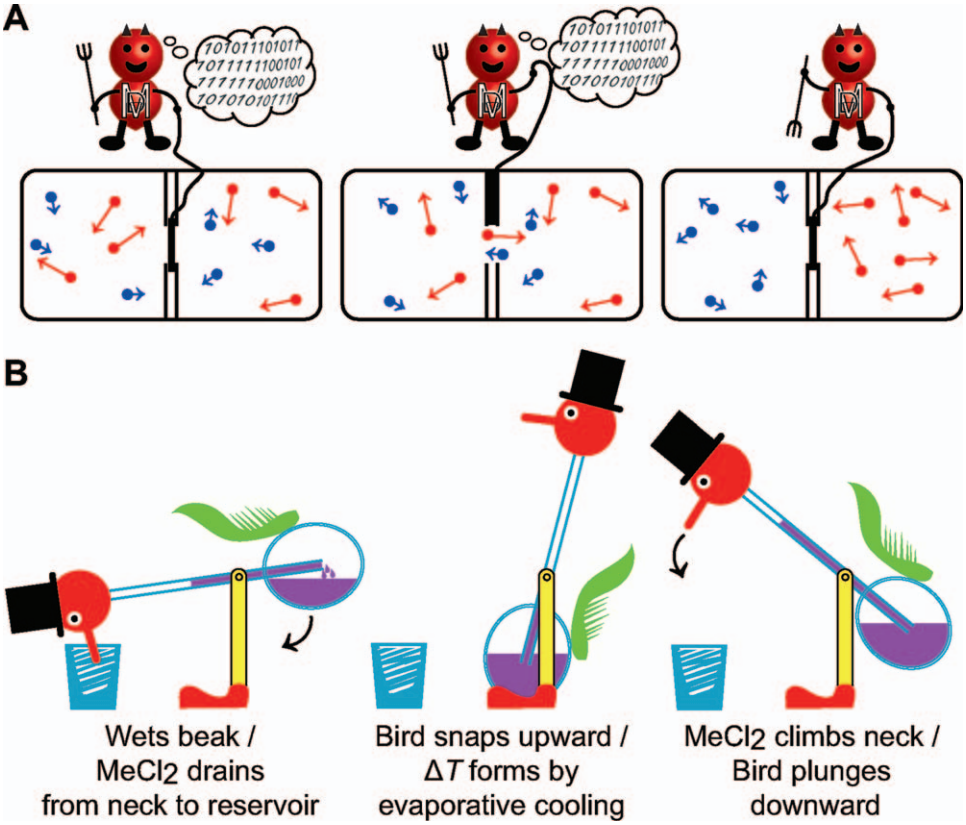

Figure 1. Real and imagined heat engines and pumps. (A) Maxwell's demon is an example of an information-powered heat pump. Left, two compartments are divided by a partition with a trap door operated by the demon. Hot (red) and cold (blue) gas atoms are shown evenly divided into each compartment. Middle and right, in order to obey the second law, the demon must consume stored information ("*101101011*...") on the individual atoms' velocities and positions, to properly sort the hot ones to the right and the cool ones to the left. (B) Thermodynamic cycle of Sullivan's drinking bird exemplifies a basic heat engine. Inertial movements of the bird are linked to the establishment and dissipation of ΔT gradients across the glass vessel body, which contains $MeCl_2$ (purple fluid). Left, when the bird dips its beak into the shot glass, $MeCl_2$ leaks from the opposite end of the tube into the reservoir, acting to ratchet the bird upward. Middle, evaporative cooling leads to $MeCl_2$ condensation. Right, $MeCl_2$ in the reservoir travels up the neck, shifting the center of mass. The bird lurches forward to complete the thermodynamic cycle.

probability of progressing rather than regressing. Directional flux is, therefore, supported by anisotropy. A perfectly symmetrical energy potential cannot support net movement in any particular direction [Fig. 2(A)]. Energy input into such a system is required in order to flash, rock, or alter the potential function. Of course, the energy input may also be used to more directly push or drive the particle (via a power stroke). However, because of the significance of diffusion and random motion at the molecular level, the ratchet-like property of the flashing asymmetrical energy potential is critical to net directional translocation. Therefore, a minimal structural feature for net motion is a physically periodic substrate and a modulated clamping interaction with the nanomachine.

Because ΔT at the required nanometer length scale is impossible to achieve inside of cells, biological nanomachines must use other kinds of energy gradients to do work. Hence the interconversion of chemical- or electrical-potential energy to mechanical kinetic energy is ubiquitous in biological molecular motors, switches, pumps, and transporters. How do nature's molecular machines perform their necessary work? As we learned from Sullivan's drinking bird [Fig. 1(B)], defining the problem facing a nanomechanical system, its environment, parts, and energy source are essential to elucidating its mechanism.

The physical environment of the cell

The environment of the cell is extraordinarily violent, where molecular movements carried out by nanomachines would be akin to sailing in a hurricane. Robert Brown initially observed the chaotic motion of pollen grains in solution; and these motions are referred to as Brownian motion. For the erratic path an individual pollen grain travels, its Brownian motion emerges statistically from the unequal number of collisions between the larger particle with many more numerous solvent molecules (having a large distribution of velocities).[14] Einstein described the average diffusion of particles of radius, r, in a solution of viscosity, η, as the mean square

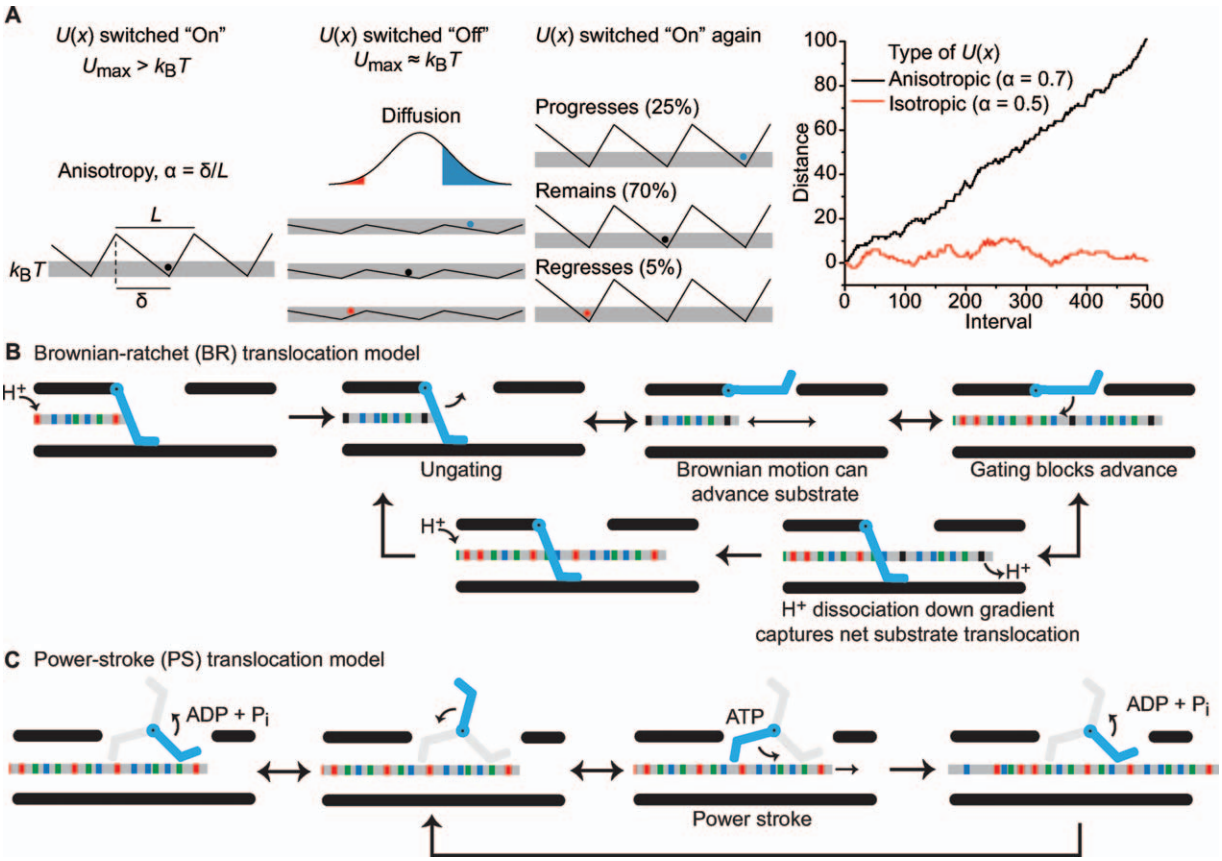

Figure 2. Molecular mechanisms of nanomachines. (A) Flashing BR model. Far left, a saw-tooth potential function, $U(x)$, with respect to distance, x, is depicted, where the positional anisotropy, α, of $U(x)$ is related to the distance between the maximum and minimum, δ, of each period, L, such that $\alpha = \delta/L$. When $U(x)$ is switched *on*, the particle is trapped in a well, since $U_{max} > k_BT$. Middle left, when the potential is switched *off*, the particles diffuse freely according to Einstein's relation. (middle right) When $U(x)$ is switched back *on*, one interval is completed and the particle is trapped again. Thus the probability of progressing is greater than regressing. Far right, a Monte Carlo simulation of the flashing BR model plotting x versus the number of switching intervals for an anisotropic (black, $\alpha = 0.7$) and an isotropic (red, $\alpha = 0.5$) $U(x)$. (B) A ΔpH-dependent BR mechanism for protein translocation. The substrate polypeptide chain is depicted as a simplistic gray rod with different functional groups colored as follows acidic (red), basic (blue), and nonpolar (green). A gate (cyan) electrostatically excludes anionic charges on deprotonated acidic residues. In this cyclical mechanism, substrate acidic residues are protonated (black); the gate opens, allowing for Brownian motion to take place. The peptide can only advance up to the point where deprotonated acidic residues enter the channel. Closing of the gate traps the peptide in the channel, as the dissipation of H^+ ions down the gradient upon deprotonation prevents retrograde movements. Further protonation then allows the cycle to repeat. (C) An ATP-dependent PS mechanism for protein translocation. The substrate chain is colored as in (B) while in this case, the gate acts more like a paddle with active (cyan) and inactive (gray) states. In the ADP-bound state, the paddle has low affinity for peptide; the paddle exchanges ADP for ATP, and subsequent ATP hydrolysis triggers a conformational change, allowing the paddle to push the polypeptide chain forward (power stroke). Cycles of ADP release and ATP hydrolysis allow the mechanism to continue.

displacement, $<\Delta x^2>$, where $<\Delta x^2> = 2Dt$: t is the time; the diffusion constant, D, is k_BT/β; and β, the frictional coefficient, is $6\pi\eta r$.[15] Thus given equal thermal energy inputs, larger objects diffuse slower than smaller ones. While macroscopic forces, F, are largely inertial and depend heavily upon mass, m, and acceleration, a, (i.e. $F = ma$), Langevin noted that microscopic Brownian particles experience a noisy, fluctuating force, ζ, which he called the "complementary force."[16,17] The fluctuating force arises from a barrage of solvent molecules colliding with the Brownian particle, and it allows an instantaneous force to be assessed for a single particle. Langevin hypothesized forces are related to velocity, v, the frictional coefficient, and fluctuating force by $F = -\beta v + \zeta$. For nanomachines, forces scale to surface area and not volume. For any single molecule, ζ can be quite significant, hence the random, unpredictable nature of any individual Brownian walk.

The behavior of polymers in solution is especially relevant for nanomachines that unfold and translocate proteins. From statistical mechanics, an unstructured protein has many more degrees of freedom than a simple, rigid Brownian particle. A

peptide backbone in the unfolded state can be assumed to have 3 degrees of freedom per amino acid, considering relevant ϕ/ψ-angle conformations. The multiplicity, W, of this peptide system, given as $W = 3^N$, translates into a configurational entropy, S, of Nk_B ln 3. Therefore, a polypeptide with $N = 50$ residues has a thermal energy of $\sim$33 kcal mol^{-1} ($\sim$140 kJ mol^{-1}). These energies are much more significant for the polymer relative to a simple, rigid Brownian particle, which experiences only three translational degrees of freedom.

Molecular mechanisms of biological nanomachines

Generally, two competing mechanisms describing the functionality of nanoscale molecular machines have been presented[18] [Fig. 2(B,C)]. On one hand, nanomachines falling into the Brownian-ratchet (BR) classification do work by using external energy sources to harness Brownian thermal energy [Fig. 2(B)].[13,19-21] A Brownian ratchet on the biological scale is analogous to a Smoluchowski-Feynman ratchet and requires an external gradient as an energy source. Imagine a nanomachine acting on an unfolded polypeptide chain with sites that can be modified to be in permissive and nonpermissive states [Fig 2(B)]. The ratchet can switch between the permissive *on* and nonpermissive *off* states through the modification of the substrate, in this case by protonation. Analogously, a gate in the transporter switches to a permissive *open* or nonpermissive *closed* state, depending on the protonation state of the polymer. Under the influence of a chemical gradient (e.g. a proton gradient, ΔpH) residues may be more likely to be in a permissive state on one side of the membrane than on the other. Thus translocation can proceed in the direction of nonpermissive modification, since nonpermissively modified substrate will be unable to retrotranslocate. A number of chemical modifications have been suggested to follow such a mechanism. Protonation,[21,22] chaperone binding,[23,24] glycosylation, disulfide bonding, and conditions that promote protein folding[19] are all capable of biasing movement through a translocase channel.

On the other hand, the power-stroke (PS) classification suggests that molecular machines use external energy sources to directly drive motion without the need for harnessing Brownian thermal fluctuations [Fig. 2(C)].[25] The binding of ATP, for example, induces a conformational change in the protein machine that performs useful work such as pulling or pushing a substrate through the translocase. The machine engages with the translocating polypeptide chain via a polypeptide clamp or other active site loop structure. ATP hydrolysis and release of ADP and inorganic phosphate (P_i) allows the machine to return to its original conformation. However, the resetting of the polypeptide clamp or other active-site structure must occur via a different path back to the initial state, else it would essentially undo the work done in the ATP binding step.

The major difference between the BR and PS models is that the latter does not consider Brownian thermal fluctuations (or Langevin's random force, ζ) to be part of the mechanism. However, BR and PS mechanisms should not be held as mutually exclusive models. Instead, these two types of mechanisms may occur at distinct junctures in the transport cycle. For example, the two-headed motor, kinesin, uses an ATP-driven PS to nudge the trailing leg forward; however, this push provided by ATP binding is far too small to drive the leg the 8 nm span between binding sites on the microtubule, and a BR phase is required to bridge the remaining distance by allowing the head to diffuse and seek its next binding site, thus completing the transport cycle.[26] Furthermore, as operating on polymers in a cell is akin to sailing in a hurricane, consider two readily available types of machinery for hoisting up a sail: a simple hand crank and a hand crank with a ratchet. Under ideal conditions, the crank driven by a PS may suffice in performing the task. However, under tropical cyclone conditions, a system that includes both a PS-driven crank and a ratchet may become necessary. While extremely windy and diffusive weather likely makes it difficult for the sailor to turn the simple hand crank in the proper direction, the ratchet ensures that substeps of a crank cycle are not lost to diffusive backsliding.

Anthrax Toxin as a Protein Translocation Model System

In this review, we focus on protein pumps or translocases that move proteins within the cell. These nanomachines consume energy in order to disassemble and translocate folded polypeptide substrates. They are found both in solution and in lipid bilayer membranes. The former serve the cell as disaggregases, protein complex disassembly machines, and unfoldases that aid in intracellular protein degradation.[27-29] The latter allow proteins to be transported either across or into lipid bilayers.[1,2,4] The binary A/B bacterial toxins[30]—including diphtheria, botulinum, and anthrax toxin—are a widely studied class of membrane transport systems, which use their own transport machinery to enter cells.[31-33] These A/B toxins assemble into complexes on cell surfaces and then utilize host cell chemical potentials to unfold and translocate enzymatic factors into the host cell.

Anthrax toxin, the binary A_2B toxin[31] produced by *Bacillus anthracis*,[1,34] [Fig. 3(A)], represents an attractive model system for probing the molecular mechanism of protein translocation across membrane bilayers for a variety of reasons. First, its three protein components can be expressed recombinantly and studied independently. Second, the

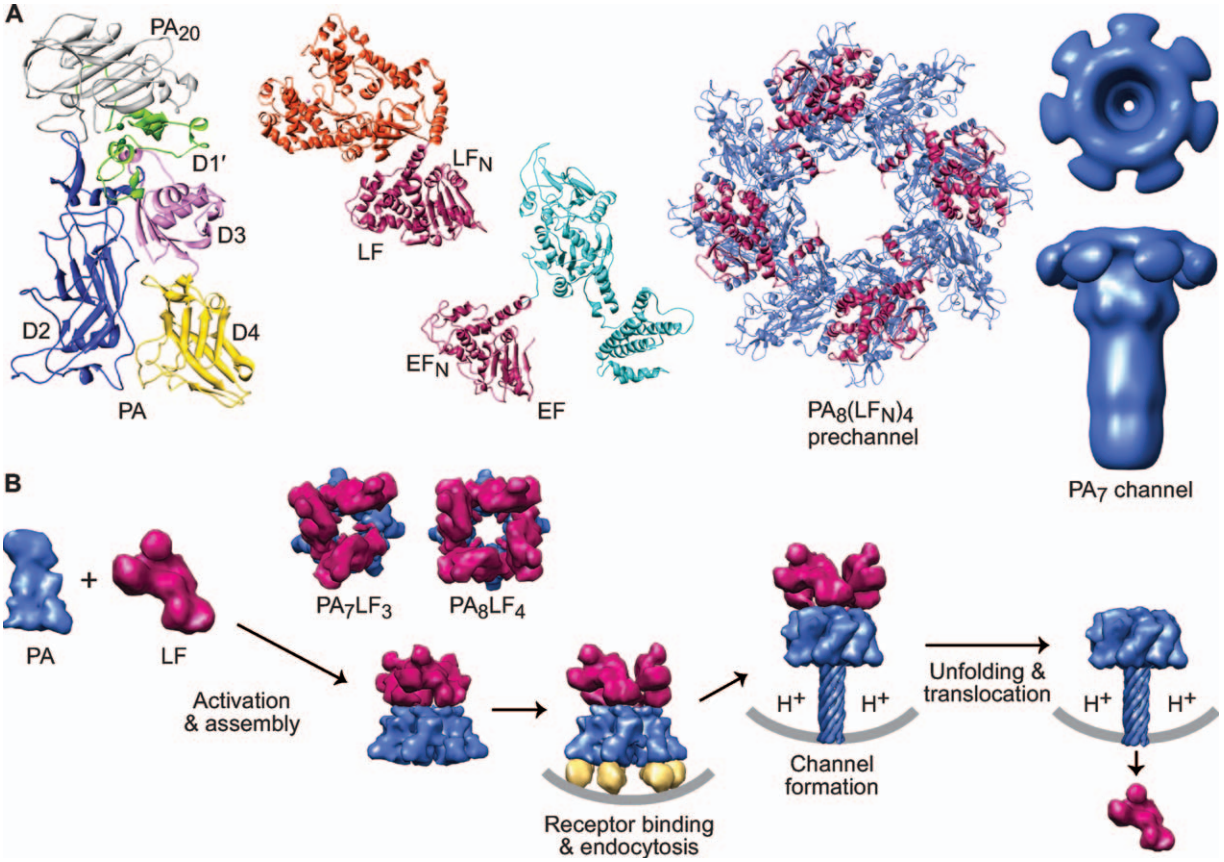

Figure 3. An overview of the anthrax toxin protein translocation system. (A) Components of anthrax toxin (left to right). Ribbons depiction of PA (3TEW[35]) colored by domain: PA_{20} (gray), D1′ (green), Ca^{2+} ions (dark green), D2 (blue), D3 (magenta), and D4 (yellow). The enzymes, LF (1J7N[36]) and EF (1YOV[37]); their amino-terminal PA binding domains (LF_N and EF_N, respectively) are colored red-violet and their catalytic domains colored orange and cyan, respectively. A representative PA prechannel complex, $PA_8(LF_N)_4$, (3KWV[38]); the PA oligomer and LF_N colored denim and red-violet, respectively. Axial view (above) and sideview (below) of a three-dimensional EM reconstruction of the PA_7 channel[39] (colored denim) (Prof. Mark Fisher graciously provided the EM density map). (B) Anthrax toxin assembly and transport. PA (denim) is proteolytically nicked and assembles with LF (red-violet) and forms PA_8LF_4 and PA_7LF_3 prechannel complexes[40,41] (based on 3KWV[38] and 1TZO,[42] respectively). Prechannel complexes bind cellular receptors (gold; 1T6B[43] and 1TZN[44]) triggering endocytosis; acidic pH conditions in the endosome induce PA to form a transmembrane channel[39,45,46] (atomic model 1V36[47]); the pH gradient that develops across the endosomal membrane destabilizes LF,[48] drives LF unfolding[22,49] and translocation[21,22] through the PA channel.

protein translocase and the individual steps of substrate translocation can be readily reconstituted from purified proteins and studied using planar bilayer electrophysiology at the ensemble[21,22,38,49,50-58] and single-molecule level.[22,40,49,51,59] Critical to this electrophysiological approach (also used in other systems[60-67]) is the ability to precisely control the driving force and solution conditions on either side of the membrane. Third, for a membrane-protein system, structural studies using X-ray crystallography are tractable, because the translocase also exists in a soluble state.[38,40,42,68] In this manner, researchers have been able to obtain structural information[35,36,38-40,42,68-70] and distinguish possible translocation models using a wide variety of functional assays.[21,22,38,49-58,71]

The structures of the three anthrax toxin components are known [Fig. 3(A)]. The protective antigen (PA) component, which forms the translocase channel, is secreted as an 83 kDa proprotein.[68] The other two components that are transported by PA are ~90 kDa enzymes, lethal factor (LF),[36] and edema factor (EF).[70] In order for the toxin to function, PA must first be proteolytically nicked by a furin-family protease,[72,73] releasing an amino-terminal 20 kDa fragment, PA_{20}. The resulting 63 kDa fragment can assemble into an active holotoxin complex comprised of multiple copies of LF and EF bound to a ring-shaped PA oligomer [Fig. 3(B)]. There are two known PA "prechannel" oligomeric architectures, a homoheptamer (PA_7)[42,68,74] and a homooctamer (PA_8).[38,40,75] The assembly and binding interactions between the PA oligomer and its substrates are well characterized.[38,76-81] Currently only one crystal structure is known of a prechannel core complex, $PA_8(LF_N)_4$, where LF_N is the PA-binding domain of LF [Fig. 3(A)].[38] These prechannel complexes either assemble on cells by binding a specific protein receptor[82,83] or localize to cells after

assembling in the plasma.[75] Internalization and subsequent acidification within the endosomal compartment converts PA prechannels into membrane-embedded channels,[45,84,85] which are strongly cation-selective.[46]

The acidic environment of the endosome is required for the action of the toxin,[86] and it generates a proton motive force (PMF) comprised of both a chemical potential (ΔpH) and an electrical potential (Δψ) capable of driving LF/EF unfolding[22,48,49] and translocation.[21,22,48,49,52] Translocation initiates from the amino terminus of LF,[87] albeit a cationic unstructured amino terminus is sufficient for initiating translocation.[38,88] The ΔpH component of the PMF is sufficient to unfold and translocate proteins.[22] Moreover, while either the ΔpH or Δψ is sufficient to translocate both LF_N and the amino-terminal PA binding domain of EF (EF_N) the translocation of the physiological full-length LF and EF substrates requires the ΔpH more so than the Δψ.[21] The molecular mechanism of ΔpH-driven translocation is believed to be consistent with a charge-state BR model,[21,22,53,54,89] where differential protonation of anionic charges in the substrate polypeptide are essential for transport[21,22] [Fig. 2(B)]. In support of the charge-state BR model, ΔpH-driven translocation depends upon charged residues[53,54] and, more precisely, acidic residues[22] in the translocating protein sequence.

PA Channel

Recent reports have provided insights into the structure of the PA translocase both in its soluble prechannel state and its membrane-inserted channel state. Many studies have shown that PA forms PA_7 oligomers, mostly due to the nature of the preparation used.[42,68,74] When PA co-assembles with either of its substrate proteins, PA oligomerization turns out to be much more complex and heterogeneous. Under these conditions, PA forms mixtures of PA_7 and PA_8 oligomers in solution and on cell surfaces.[40] The PA_8 oligomer can carry a maximum payload of four LF or EF molecules, while the PA_7 oligomer can carry a maximum payload of three substrates [Fig. 3(B)].[38,40,41] Despite a slight increase in the internal diameter of the oligomeric ring and a corresponding increase in the single-channel ion conductance of the PA_8 oligomer relative to the PA_7 oligomer, the change in channel diameter appears to have a very subtle impact on the translocation mechanism.[40] The PA_8 oligomer, however, has the advantage of increased thermostability relative to the PA_7 oligomer, where the added interdomain contacts and surface burial in PA_8 oligomer provide additional stabilizing contacts.[40,75] Thus the more stable PA_8 oligomer is less sensitive to premature channel formation under physiological temperature and pH conditions.[75] This stability difference, however, is not observed when either PA oligomer is bound to the extracellular domain of its host cell receptor, and the receptor domain effectively stabilizes PA_7 and PA_8 oligomers through a similar mechanism.[42,45,90] A recent study described a molecular mechanism for PA oligomer stoichiometry.[35] The interface between PAs domain 2 and domain 4 (D2-D4) controls the relative proportions of the PA_7 and PA_8 complexes that form as PA assembles, and the D4 domain natively adopts pro-PA_7 and a pro-PA_8 conformations in ~3:1 ratio.[35] The octamer has also been exploited as structural tool for crystallographic studies due in part to the architecture's increased thermostability and internal symmetry.[38,40]

Using electron microscopy (EM), the structure of the PA_7 channel has been recently imaged [Fig. 3(A)].[39] The PA channel is mushroom-shaped and approximately 170 Å tall × 125 Å wide at its maximum dimensions. The wider, cap-shaped part of the structure is about 70 Å long and likely contains the LF/EF binding sites. Beneath the cap is a 100 Å long stem, which is likely a 14-strand β-barrel structure; the stem ultimately inserts into and spans the membrane bilayer.[69] Earlier electrophysiology studies suggested the stem is an extended β-barrel structure.[91] From basic modeling studies,[48] the β-barrel stem is likely only able to accommodate structures as wide as an α helix (10–15 Å wide); therefore, LF and EF must unfold during translocation.

The PA translocase channel can be divided into three sections (Fig. 4): the substrate docking surface in the cap (called the α-clamp site), a critical hydrophobic constriction point about one-third of the distance into the translocase (called the ϕ-clamp site), and the highly charged solvophilic β-barrel stem portion, which comprises the bottom two-thirds of the translocase. Interestingly, there appears to be separate polypeptide interaction sites, or clamps, associated with these different points in the PA translocase channel. These clamps also allow the channel to interact with the substrate nonspecifically. We consider the notion of a clamp to more closely resemble a dynamic binding site for polypeptide, where, for example, a clamp site can be modulated from a higher-affinity binding mode to a lower-affinity binding mode. This dynamic is critical to allowing the translocase to both favor unfolding and translocation while preventing tight binding interactions from occurring that would otherwise impede transport. In the following sections, we will summarize these clamp structures and their associated activities.

The α clamp

Recently, the structure of $PA_8(LF_N)_4$ was reported, providing a molecular description of the interaction between the PA oligomer and LF_N.[38] LF binds to PA in two distinct subsites: a carboxy-terminal subsite comprised of specific interactions and an unconventional binding cleft formed at the interface of adjacent PA subunits, called the "α clamp." Interestingly, in the

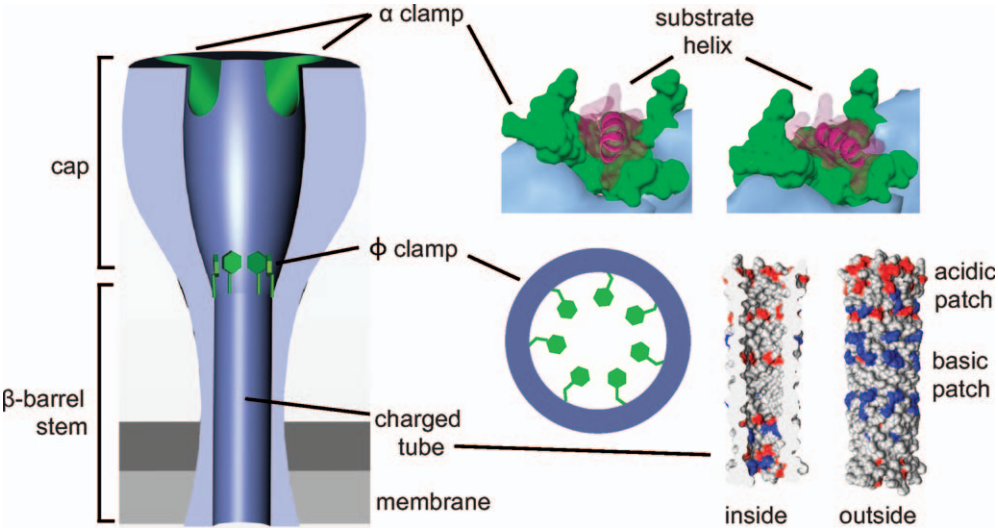

Figure 4. Peptide clamps in the PA channel. The PA channel (denim) contains clamping sites (green) and a β-barrel tube with positively (blue) and negatively (red) charged patches. Partially unfolded substrates (red-violet) first bind to the α-clamp site.[38] Subsequently, the peptide threads into the ϕ clamp, which is comprised of a ring of F427 residues.[52] Finally, the substrate polypeptide chain encounters the β-barrel tube,[91,92] which may act as a putative charge clamp, attracting cationic sequence and preventing the retrotranslocation of deprotonated acidic residues.

complex, LF_N α1 and β1 unfold from their native conformation and dock into the α-clamp subsite on the surface of the PA_8 oligomer [Figs. 4 and 5(A)]. PA R178 forms contacts with LFs α1 and suggests an electrostatic capping interaction with the negative dipole of the carboxy-terminal end of α1. The interaction has been extensively verified to occur in the prechannel and channel configuration of PA.[38,71] Furthermore, the partial unfolding of LF_N upon binding PA is relevant to toxin assembly, as PA prechannels are produced less efficiently when co-assembled with an LF_N construct lacking its α1/β1 structures.[38]

The manner in which the α clamp interacts with LF_N's α1/β1 explains why the site is well equipped to recognize protein sequence in a nonspecific manner.[38] Structurally, PA's EF-hand-type twin Ca^{2+}-binding sites frame the cleft and provide a structural scaffold consistent with how calmodulin complexes bind to peptide helix substrates [Fig. 5(B)].[93,95] In this manner, the residues lining the site coordinate the Ca^{2+} ions, leaving their backbone atoms to form much of the interacting surface with the unfolded structure. Overall, LF_N α1/β1 excludes 1000 $Å^2$ of solvent accessible surface area (SASA) on PA. Functional studies show the α-clamp-LF_N interaction is worth ~2.5 kcal mol^{-1}, and this thermodynamic stability is largely invariant with sequence.[38] Interestingly, PA α-clamp residue L203 forms two parallel β sheet-like hydrogen bonds with LF_N β1 residues. The parallel β-sheet interaction is effectively limited to two hydrogen bonds, as PA P205 prevents further β-sheet like bonds from forming. Extensive mutagenesis in LF failed to identify specific side chain interactions in the α clamp. In fact, the α1 sequence in LF can be essentially replaced with other sequences in LF and EF and still maintain essentially wild-type binding and translocation activity [Fig. 5(C)].[38] Aromatic residues F202 and F236 were found to be important for full-length LF translocation; however, neither residue plays a role in initial binding to LF_N.[38] Thus, the α-clamp site can garner significant nonspecific polypeptide binding activity using a general shape-complementarity binding mechanism, leading to the exciting prospect that helical structure in the substrate represents a key handle for the translocase to grip its substrate during translocation.

The co-crystal structure of $PA_8(LF_N)_4$ provides a first-time look at the process of protein unfolding on the surface of an unfolding machine [Fig. 5(A)].[38] Since more than half of the total binding interface is attributed to recognizing LF_N's unfolded α1/β1 structure, it would appear that substrate unfolding is required to obtain tight binding to the PA oligomer. This unfolding requirement is indeed the case, as the substrate's affinity for channels is reduced 10^4-fold when unfolding is prohibited by covalently linking α1 to the main body of LF_N with a disulfide bond.[38] Furthermore, solution studies probing the degree of LF_N unfolding revealed that the substrate is effectively destabilized by ~1 kcal mol^{-1} upon binding to PA. It is still unclear to what degree the protein becomes destabilized on the surface of the PA oligomer; however, decreases in fluorescence anisotropy and inversely proportional increases in

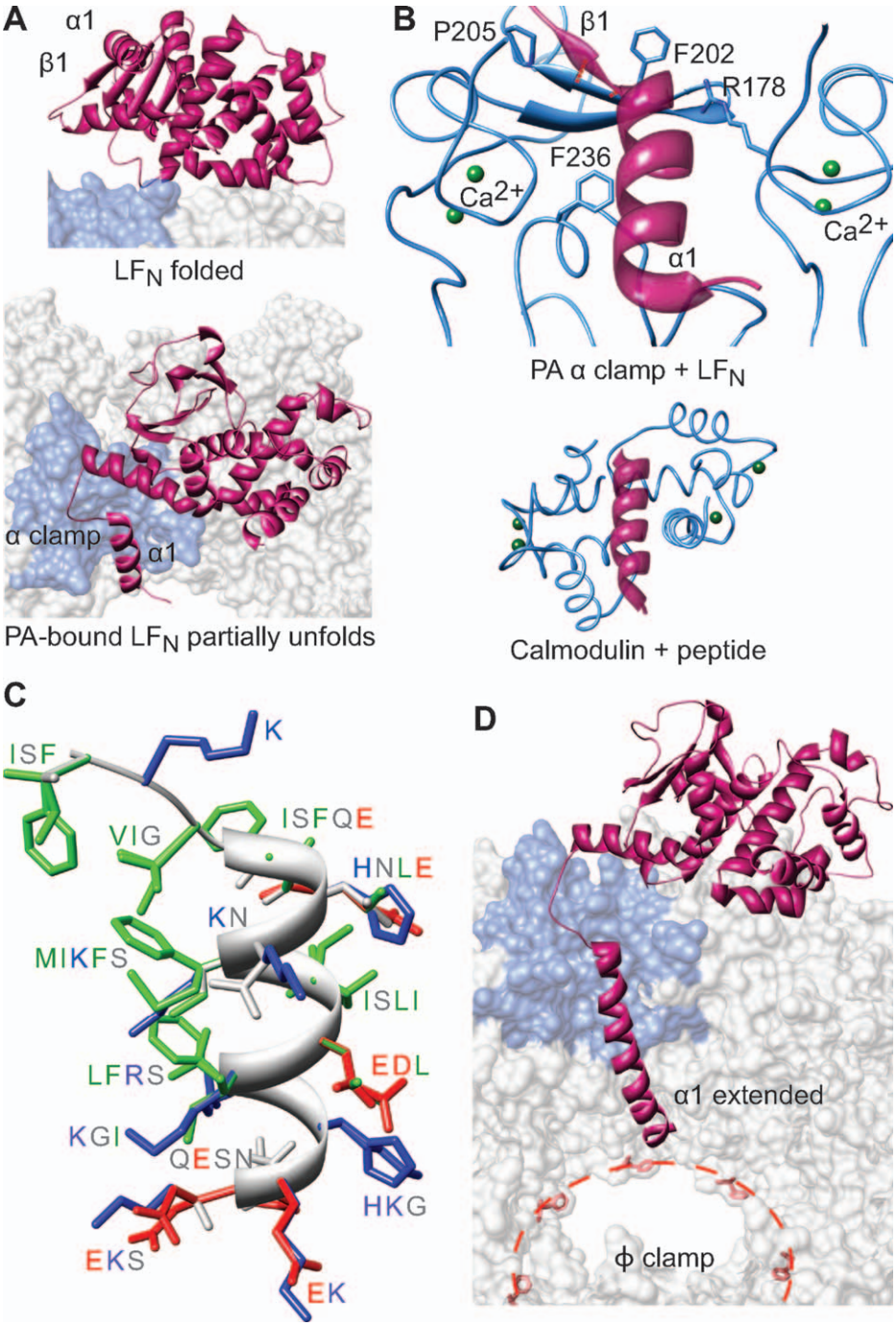

Figure 5. The α clamp. (A) LF_N (red-violet) changes conformations from (top) a folded (1J7N[36]) to (bottom) a partially unfolded (3KWV[38]) state, such that LF α1/β1 unfurl and bind into PA's α clamp (denim surface). (B) Top, a detailed view of the α clamp (denim ribbon) in complex with LF's α1 (red-violet ribbon) indicating the structural calcium ions (green) scaffolding the site. Bottom, calmodulin in complex with a peptide helix (1CDM[93]), where the latter is colored analogously to the α-clamp structure. (C) The α clamp can bind nonspecifically to and translocate a variety of sequences illustrated in a helical structural alignment, which is colored by residue chemistry: basic (blue), acidic (red), polar (gray), and hydrophobic (green).[38] (D) Considering the Zimm-Bragg formalism,[94] the α clamp may act as an α-helix nucleation site. Elongated helical structure can then be fed into the ϕ clamp (red dotted line and F427 residues).

atomic displacement parameters (*B* factors) have been observed in the substrate when it binds the PA oligomer. Thus, while 2.5 kcal mol^{-1} of binding stabilization is derived from the docking of LF_N into the α clamp, the remaining folded protein is destabilized by at least 1 kcal mol^{-1}. This value potentially represents a destabilization minimum, given the degree of disorder introduced into the body of the protein. The nonspecific binding activity of the α-clamp site is likely critical to the channel's ability

to unfold and translocate multidomain substrates, like full-length LF.

The ϕ clamp

The acidified endosomal trafficking route produces conditions that thermodynamically destabilize the substrates, LF and EF, causing them to populate molten-globule intermediates.[48] To determine how LF and EF are linearized and fully unfolded during translocation, a series of experiments were performed to identify potential active-site residues lining the PA channel.[52] An interesting conserved residue, F427, was identified in an otherwise hydrophilic PA loop, N^{422}AQDD**F**SSTP. As most of the channel-lining residues are hydrophilic and/or anionic,[89,91] this aromatic site is unusual in terms of its chemistry and prominence in the interior of the PA channel. Structurally, each PA subunit contributes one F427 residue, and the collective ring of aromatic rings forms a hydrophobic bottleneck in the PA channel. The site, dubbed the "ϕ clamp," is critical for translocase function (Fig 4).[52] Analogous ϕ-clamp sites have been identified in numerous protein translocases, including soluble ones that hydrolyze ATP,[96] revealing the general importance of the site to the mechanism of translocation.

PAs ϕ clamp has been characterized extensively by numerous biophysical techniques to better understand the molecular mechanism of translocation. The F427 residues radially converge within the channel, forming a symmetric ring of rings, which is very narrow. Single-channel electrophysiology studies confirmed that the ϕ clamp forms a conductance bottleneck (or constriction point) within the channel. As the ion conductance path and the protein translocation path are the same, it is unsurprising that defects arising from mutations to the ϕ clamp manifest in increased substrate diffusion, backsliding, and retrotranslocation. The retrotranslocation phenotype of these ϕ-clamp mutants likely explains their >1000-fold losses in translocation activity;[52] moreover, the ratchet-like behavior of the ϕ clamp indicates it is a dynamic clamping site, allowing translocation to proceed in one direction but opposing backsliding in the opposite.

The ϕ clamp has broad substrate specificity with preference for hydrophobic aromatic compounds.[52] The broad specificity is consistent with the π-cloud electrons of the Phe residues making cation-π, π-π, and π-dipole interactions. Recent reports[57] indicate substitution of a single Phe residue in the ϕ clamp with a charged residue fully inactivates the translocase, which is consistent with a cooperative site. Since the hydrophobic effect generally exhibits a high degree of cooperativity in protein folding studies,[97-99] it is reasonable to hypothesize that the ϕ clamp is a hydrophobic interaction site, operating similar to a protein chaperone, where the site interacts with a broad spectrum of peptide chemistries during translocation.

An analysis of known prechannel oligomeric crystal structures reveals that the ϕ-clamp loop is quite flexible and exists in two different conformations.[38,40,44] In the ligand-free structure of PA_8 (Protein Data Bank 3HVD),[40] both the ϕ-clamp loop and the hydrophilic loop containing K397, located directly above the ϕ-clamp loop, are tilted upward, relative to the $PA_8(LF_N)_4$ structure (3KWV)[38] and the PA_7 structure (1TZO).[42] Interestingly, it appears as if the conformations of the two loops are coordinated, since a K397 loop in the *down* conformation would sterically clash with a ϕ-clamp loop in the *up* conformation. While these structures are of PA prechannels, some evidence supports the functional implications of coordinated loop movement.[100] A mutagenesis study of K397 and D426 found that these residues may make a salt bridge upon channel formation.[100] This salt bridge linking these two flexible loops may position the ϕ clamp in an active conformation,[100,101] or the different configurations observed may be alternative binding modes of the ϕ clamp, that is, a high affinity and a lower affinity state of the site. Proton binding may be able to modulate the salt-bridge interaction, altering the substrate affinity of the ϕ clamp site.

The β barrel

The length, diameter, and electrostatic composition of the PA channel and its extended β-barrel stem likely play a key role in the molecular mechanism of translocation (Fig. 4). While an atomic-resolution structure of the PA channel is currently unavailable, a β-barrel model[47] has been proposed.[91,92] EM studies also show a tube-like stem consistent with a β-barrel architecture.[39,69] The β barrel's inner diameter is no wider than the width of an α helix[48] and may stabilize helical structure due to favorable van der Waals contacts and backbone desolvation. A number of charged residues populate both the inside and outside of the β barrel. These charges create patches of alternating electrostatic potential within the barrel (Fig. 4). The precise role of the charged groups in the barrel is unknown; however, the charge-state BR mechanism [Fig. 2(B)] proposes that differential electrostatic repulsion between the channel and substrate polypeptide is critical to the overall mechanism of ΔpH-driven translocation.

Translocation Powered by a ΔpH

The PA translocase machine is powered by the chemical potential component, ΔpH, of the PMF.[21,22] While a pure Δψ can drive the translocation of LF's amino-terminal domain, LF_N,[50] the ΔpH is required for the translocation of the full-length substrates, LF and EF,[21] and a ΔpH alone is sufficient for translocation.[22] A charge-state BR model was initially

proposed for the molecular mechanism of ΔpH-driven translocation [Fig. 2(B)].[21] The model is based on the fact that the PA channel itself is cation-selective (or anion-repulsive),[46] and yet LF and EF are anionic substrates with isoelectric points of 5.4 and 6.6, respectively (more importantly, their amino-terminal domains, LF_N and EF_N, have p*I* values of 4.9). Krantz *et al.* proposed that this paradox is resolved if acidic residues can be protonated during their translocation through the PA channel, thereby allowing their anionic charges to be neutralized.[21] The ΔpH naturally favors substrate protonation on the endosomal side of the membrane, where the pH is ~5.5, but once the substrate reaches the higher pH side of the membrane (neutral cytosolic pH), these acidic residues would spontaneously deprotonate. Thus, while these protonated acidic residues could pass through the channel's cation-selective filter, they would be trapped on the opposite side of the membrane upon substrate deprotonation. In this mechanism, substrate motion is largely explained by Brownian motion, and the ratchet is an electrostatic trap created via cycles of acidic residue protonation and deprotonation on either side of the channel's charge-selectivity filter.

Several recent studies support the charge-state BR model of translocation. In one study, it was shown that sulfate groups attached to LF_N via cysteine linkage inhibited Δψ-mediated translocation.[56] Since the sulfate moiety essentially cannot be protonated under the experimental conditions, the authors concluded that only titratable negative charges could pass through the cation-selective channel. Another study reached a similar conclusion by incorporating cysteic acid residues in a semisynthetic LF_N construct.[54] Furthermore, semisynthetic LF_N constructs lacking titratable acidic residues in the amino-terminal presequence display significant translocation defects.[54] A recent report extensively probed the role of both positively and negatively charged residues in LF_N's presequence.[22] Interestingly, substrates lacking acidic residues could be translocated by a Δψ alone, yet they do not display ΔpH-dependent translocation. This evidence strongly supports the model that the ΔpH drives translocation by protonating acidic residues and is consistent with the charge-state BR model. Furthermore, it was demonstrated that basic residues likely act as chaperones for deprotonated acidic residues. That is, segments of sequence containing high densities of negative charge will not enter the PA channel as efficiently as those containing positively-charged residues nearby.

The ΔpH plays a role not only in translocation but also in the unfolding of the substrate. As discussed above, the thermal energy of even a small polypeptide is quite large (over 100 kJ mol^{-1}) and, if properly rectified, can lead to significant force generation (tens of piconewtons), which is sufficient to accelerate the protein unfolding process. The most ΔpH-dependent step of translocation is associated with the protein folding barrier,[49] which is consistent with the observation that a ΔpH alone is sufficient to unfold and translocate a fully folded substrate.[22] Furthermore, acidic residues in LF_N are naturally concentrated in an optimal position immediately before the substrate's folded domain and separating this region of optimal charge density from the folded domain greatly inhibits translocation.[22] Taken together, these results imply a model for ΔpH-dependent unfolding. As the substrate presequence is translocated and captured on the high pH side of the membrane, the remainder of the polypeptide is caught in an extended state with more limited conformational options. This results in entropic tension that is only relieved via substrate unfolding.

Translocation-Coupled Unfolding

The narrow architecture of the PA translocase channel necessitates that substrates must unfold before translocation. Critical to understanding protein translocation is determining how driving forces are coupled to substrate unfolding. Thoren *et al.* probed the folding step by site-directed mutagenesis, thermodynamic stability studies, and planar lipid bilayer electrophysiology.[49] The ΔpH- or Δψ-driving-force dependencies of the activation energy of translocation ($\Delta G‡$) revealed a boomerang-shaped curve with two distinct limiting slopes. At low driving force, the $\Delta G‡$ is 10-fold more force dependent than at high driving forces. Thus two major barriers are crossed during translocation: one that is strongly force-dependent and one that is largely force-independent. Thoren *et al.* were then able to show that substrate unfolding occurs at the more force-dependent barrier and little unfolding occurs at the more force-independent barrier.[49]

By examining destabilizing mutations throughout the substrate protein's structure, the location of the folded substructure that is rate-limiting to the unfolding step of translocation was identified. For LF_N, the substrate's β-sheet subdomain corresponds to this "mechanical breakpoint" region. β-sheet regions often represent the rate-limiting mechanical breakpoint in a force-dependent unfolding mechanism, as probed by optical force microscopy; and the orientation and topology of β-sheet substructures are key determinants of the forces required for unfolding.[102] Interestingly, the β-sheet substructure region is less ordered for PA-bound LF_N relative to unbound LF_N.[38] Thus, the unfolding of LF α1/β1 upon binding essentially lowers the activation energy required to unfold the substrate, as strain and disorder is pinpointed at the mechanical breakpoint site.

Finally, because so little unfolding appears to occur in the less force-dependent step, it has been proposed that this step is limited by the translocation of the unfolded chain.[49] The translocation barrier by its nature of having a shallow force dependence cannot be reduced significantly and places an overall speed limit on the rate of protein translocation for anthrax toxin[21,49] and other systems.[103-105] Despite the fact that other translocases use ATP as their source of free energy, it appears the translocation step is bottlenecked in the range of ~1 to 10 s for protein substrates that range in size from 100 to 800 residues in length. Most likely, this bottlenecking limits the ultimate rate of translocation and reflects that the overall force-independence of the postunfolding event is a general feature in many systems.

A different model proposed by Basilio *et al.* proposes that translocation is not a barrier-limited process but rather an electrodiffusive movement of a "charged rod" through the channel.[51] By definition, this particular model does not consider unfolding during LF translocation to be rate-limiting. It is difficult to reconcile this model with the majority of published studies on protein unfolding, which show, in fact, that unfolding is barrier limited[106] and force-dependent.[102,107-109] Force along the translocation axis of a membrane-embedded translocase are readily achieved for charged ions, q, in an electric field, E, by $F = Eq$. Similarly, optical force-microscopy measurements of substrate proteins being pulled through ATP-dependent unfolding machines show significant barriers to unfolding, where the most force-dependent step is related to unfolding.[110] Thus studies of soluble ATP-dependent unfolding machines agree more closely with the conclusions of Thoren *et al.*[40] and are less consistent with the charged-rod hypothesis proposed by Basilio *et al.*[51]

Processing Unfolded Protein: Challenges and Solutions

The nature of unfolded polypeptide presents significant complexities and challenges for the nanomachine, including: (i) chemical complexity;[38,52,111] and (ii) configurational complexity, diffusion, and orientation.[38,49] By contrast, the nanomachine kinesin moves along a very specific polymer track, a microtubule. The regular chemical periodicity of microtubule tracks provides convenient, highly organized highways for kinesin to transverse.[7] Dealing with the chemical and configurational complexity of an unfolded protein polymer implies that the fundamental challenge the translocase faces is entropic in nature. In order to do work on a reasonable timescale, protein translocases must contend with entropy.

The catalytic power of orienting substrates in an enzyme reaction was initially described by Page and Jencks, where enzyme catalyzed rates are accelerated by the appropriate orientation of reactive chemical groups.[112] This orientation effect, referred to as an "entropy trap," was considered to be critical to the observed rate accelerations of enzyme-catalyzed reactions. The entropy trap results from the exchange of enthalpic interactions in an enzyme's active site binding pockets with the substrates; these binding interactions can reduce the overall rotational and translational degrees of freedom and accelerate the chemical reaction. The individual chemical steps of anthrax toxin translocation are protonation, deprotonation, and translocation [Fig. 2(B)]. It is likely these steps require oriented and somewhat ordered substrates, thereby reducing the conformational search and subsequently lowering the $\Delta G^{\ddagger}$ for each reaction. Efficient, well-designed protein translocases are enzyme catalysts, and as such, they would tend to maximize ordered motion, and minimize heat dissipation, to the greatest extent possible and within the limits of the Second Law. As concluded by Jencks, the more an enzyme minimizes counterproductive motions of its substrate, the more significant acceleration in catalysis is realized.

Chemical complexity

Imagine a protein channel that is 50 to 150 Å long; during translocation, a frame of 15 to 50 residues is contained in the channel. The possible chemical complexity (considering the 20 natural amino acids) is enormous, ranging from 15^{20} to 50^{20} depending on channel length and polypeptide conformation. Therefore, it is reasonable to assume that protein translocases are not designed to *specifically* recognize each and every type of possible amino acid sequence. This type of design principle would be impossible to encode into the machine. Instead, the translocase may recognize broad structural or chemical properties of peptides. This type of sequence recognition is often called "nonspecific binding," and it refers to the ability of a binding site to recognize substrates using general features of the polymer. Even in the case of anthrax toxin—which only has two known natural substrates, LF and EF—the PA translocase is highly nonspecific and capable of translocating heterologous sequences.[38,88,113,114] This nonspecificity comes as no surprise, given that the frame of sequence within the machine is continuously changing during translocation. Here we consider two classes of mechanisms that the anthrax toxin protein transporter system exploits in addressing the issue of nonspecificity:

- Class I: Hone in on general sequence properties, namely patches of sequence dense in hydrophobicity (i.e. sequence hydropathy) and/or a particular type of charge.
- Class II: Bind nonspecifically to sequences with similar steric shape, without regard to sequence chemistry.

For the Class I mechanism, we hypothesize that the machine can effectively *average* diverse residue chemistries into mean sequence properties for a given segment of peptide, thereby minimizing chemical complexity. The likely rational behind the ϕ-clamp site is its preference for hydrophobic and aromatic groups with little or no specificity for the precise geometrical arrangements of such groups.[52] Crude estimates of polypeptide binding attribute ~1.5 kcal mol^{-1} of binding free energy to the ϕ clamp.[38] Additionally, the cation selectivity of PA implies that an anion-repulsion site resides within the channel, which repels negatively charged sequences and attracts positively charged sequences. Acidic residues in the translocating chain are responsible for ΔpH-driven translocation; however, the specific location and identity of these charges are much less critical.[22]

By contrast, the α-clamp site is structurally designed to complement α-helical shape, rather than particular residue chemistries. Only one α-clamp residue, R178, makes any significant van der Waals contacts with LF_N α1 residues; the rest of the interaction is dominated by backbone contacts. Additional backbone interactions independent of side chain chemistry include two parallel β-sheet hydrogen bonds with LF_N β1. Thus the α clamp employs a Class II mechanism of highly nonspecific binding, providing ~2.5 kcal mol^{-1} of binding free energy.[38] Furthermore, this binding energy was achieved independently of the sequence composition [Fig. 5(C)]. The α clamp is capable of binding a wide variety of sequences, including nonamphipathic ones. Also the α clamp may take advantage of the intrinsic polarity of an α helix, given that the positive polarity at the amino end of the helix is oriented towards the cation-selective channel, and the negative polarity at the carboxy end is capped by the guanadino group of R178.[38] Therefore, the α clamp derives its binding affinity from shape complementarity and a pair of backbone hydrogen bonding interactions, rather than sequence-specific polar, charged, or hydrophobic contacts.

Configurational entropy, diffusion, and substrate orientation

Assume a 10-residue peptide is recognized during a cycle of translocation, and each residue can be in the α, β, or left-hand turn conformation. Such a peptide could effectively occupy ~10^5 possible conformations. Selecting specific subsets of possible conformations to bind and forcibly move during protein translocation would require work. For example, to select 10 conformations out of 10^5 would require ~4 kcal mol^{-1} of work, independent of operating under a load. Adding chemical complexity to the system further increases the entropic penalty. Assuming the translocase requires a binary pattern of hydrophobic and hydrophilic sites within the polypeptide sequence, and as there are 10^3 possible binary patterns in a decamer, selecting 10 of these configurations would increase the required amount of work to 7 to 8 kcal mol^{-1}.

A translocase thus has two mechanisms available to offset the entropic costs of binding the decamer segment: (i) making specific enthalpic interactions and/or (ii) through the dissociation of ordered solvent. The former is a mechanism of specificity and is unlikely. Specific interactions are often weak, as they can be offset by losses of peptide-solvent hydrogen bonds or ionic interactions. For the latter, many[97,98,115] have considered that the hydrophobic effect is dominant in biomolecular interactions and is due to changes in solvation of the interacting groups. The effect is related to SASA displaced upon binding. For PA, the α clamp provides 2.5 to 4 kcal mol^{-1} of binding free energy through nonspecific binding.[38] Given the SASA apparent in the structure is 1000 $Å^2$, we can estimate that the free energy gain per unit surface area is 2 to 4 cal mol^{-1} $Å^{-2}$. This value is 5- to 10-fold less than the 20 cal mol^{-1} $Å^{-2}$ calculated from a 1023-protein metaanalysis.[116] The disparity from the observed value for PA's α clamp may be due to changes in backbone configurational entropy, lower levels of ordered solvent are released upon binding, the introduction of strain and disorder elsewhere into the system, or simply a limitation inherent to the metaanalysis calculation. In any case, we may presume that nonspecific binding interactions stabilized through a general desolvation strategy can be used to do work, namely by ordering the translocating chain for further processing and/or by reducing the stability of the substrate protein. In order to achieve these aims, ~1000 to 2000 $Å^2$ of SASA was excluded upon binding. We contend that such interactions in a translocase would benefit from a uniform substructure, such as an α helix.

Even if we assume that the thermodynamic penalty is satisfied by some other means, the kinetic search process may limit translocation. Experimentally, protein substrates with ~250 to 750 residues can translocate in ~1 to 10 s,[21,103-105,117] and thus an interesting question is whether the translocase facilitates this search process. To speed up the search, the translocase may limit the conformational space of the translocating chain to a particular structure most suitable for its active site to bind. Assume the translocase engages more or less a helical structure to produce maximum force during translocation. A Class II-type structure may be able to facilitate the formation of helical structure during translocation. According to the Zimm–Bragg model for helix formation, α-helix stability, K_N, of an N-residue peptide is given as $K_N = \sigma s^N$.[94] The initiation of α-helical structure, which is described by the

factor, σ, is the limiting step. The equilibrium constant, K_N, increases with each additional residue added to the nascent helix. Thus helix formation is a nucleation process, where the equilibrium stability of a helical substrate would be greatly enhanced by the presence of a Class II structure, in the spirit of PA's α clamp (Fig. 5). Helical structure has an additional advantage of possessing reduced conformational entropy relative to unstructured peptide, minimizing the potential for dissipative losses and allowing for a more efficient utilization of the available electrical/chemical free energy source. We conclude that helix-nucleation machinery in translocases (if oriented properly along the axis of the translocase) would provide a significant kinetic benefit to the translocation mechanism.

A Proton-Engine Mechanism for Translocation

Protons are dissipated by the PA translocase during translocation by means of the protonation and deprotonation of acidic residues in the substrate chain.[21,22] Similar to the Cl^-/H^+ antiporter, which exchanges two Cl^- ions for one H^+ ion,[118] protons are consumed by the PA translocase as a fuel to drive protein flux. How are directionality and force derived from the dissipation of H^+ ions down their gradient? In prior models, Brownian motion in the translocating protein is effectively biased by changes in protonation state of acidic residues in the protein substrate. We propose that sites like the ϕ clamp may *switch* conformation during the substrate protonation/deprotonation cycle and that this action plays a key role in governing the process of translocation. Given that a salt bridge likely positions the ϕ-clamp loop in an active conformation,[100] protonation could switch the interaction between on and off states. We envision that the necessary force is generated in this mechanism through biasing of Brownian motion, electrostatic repulsion, and the release of unfolded-state conformational entropy, ΔS_{config}, upon substrate extrusion from the channel.

In this model, the α-clamp site not only facilitates protein unfolding but also stabilizes and templates the formation of α-helical structure inside the PA channel [Fig. 5(D)]. Furthermore, the internal diameter observed and predicted for 14- to 16-stranded β barrels is a suitable steric fit for peptide helices and likely favorable to helix initiation. For example, crystal structures of protein autotransporters are comprised of a β barrel, which contain α helices from the translocating chain within the lumen of the barrel.[119,120] Why may this be important? We propose that ΔS_{config} will be much greater for a helix-to-coil transition. Thus during particular cycles of the transport pathway, the channel may maximize the amount of compact structures that form, including helical conformations. The activity of the α clamp supports this hypothesis,[38] as well as recent work measuring the minimal length of polypeptide spanning the PA channel.[55] In the latter study, it was suggested using a streptavidin-biotin intermediate-capture approach that peptide chain spans the PA channel in an entirely nonhelical, fully-extended conformation. Thus, the authors conclude that the substrate translocates in a fully-extended conformation devoid of helical structure. The streptavidin-capture data show that the rate of capture for the shortest, 33-residue probe is on the order of 1000 s, which is extremely slow, considering the 260-residue substrate, LF_N, translocates in ∼10 s. The kinetics, however, suggest the opposite conclusion that the substrate is in a more compact structure >99% of the time, where the extended state is rare (i.e., <1%). The authors further argue that longer-length substrates are less accessible to streptavidin capture because the chain will spend more time retracted in the channel. This explanation is in fact consistent with the chain experiencing a more compacted state. The compacted/coiled state is likely helical based on the Zimm–Bragg formalism,[94] the substrate desolvation activity of the upstream ϕ-clamp site,[52] the structure of the LF_N-liganded α clamp,[38] and the known Ramachandran preferences[121] for polypeptides (i.e., anything less than an extended β conformation likely resides in the α-helical Ramachandran well, as the left-hand turn conformation is rare).

We suggest the translocating chain can fluctuate between more extended and more condensed states. The only requirement of our model is that during translocation the structure of polypeptide in the channel must be more compact than that immediately following extrusion from the channel; the absolute degree of helicity is not critical, as the peptide will be confined within the channel, regardless. When the polypeptide transitions from a more constrained helical state to a less constrained state, the realized increase in ΔS_{config} is significant. We propose a proton-engine mechanism, whereby the ΔpH, ϕ clamp, α clamp, and anionic-charge repulsion site in the PA channel coordinate protein translocation (Fig. 6):

- *Step 1.* Anionic/deprotonated polypeptide loads into the upper vestibule of the PA channel by means of Brownian motion, binding into the α-clamp site as helix. The α clamp acts as a helix nucleating binding site, orienting, and feeding the growing helical chain toward the channel lumen.
- *Step 2*. The ϕ clamp switches to a *closed* position, tightly gripping the substrate polypeptide. Binding of unfolded chain at the ϕ clamp prevents backsliding.[52] The ϕ clamp impedes H^+ flow, reducing $[H^+]$ below the ϕ clamp. Acidic substrate residues above the clamp are subsequently protonated, and consequently less anionic in charge. The stability of the interaction at the ϕ clamp site may be

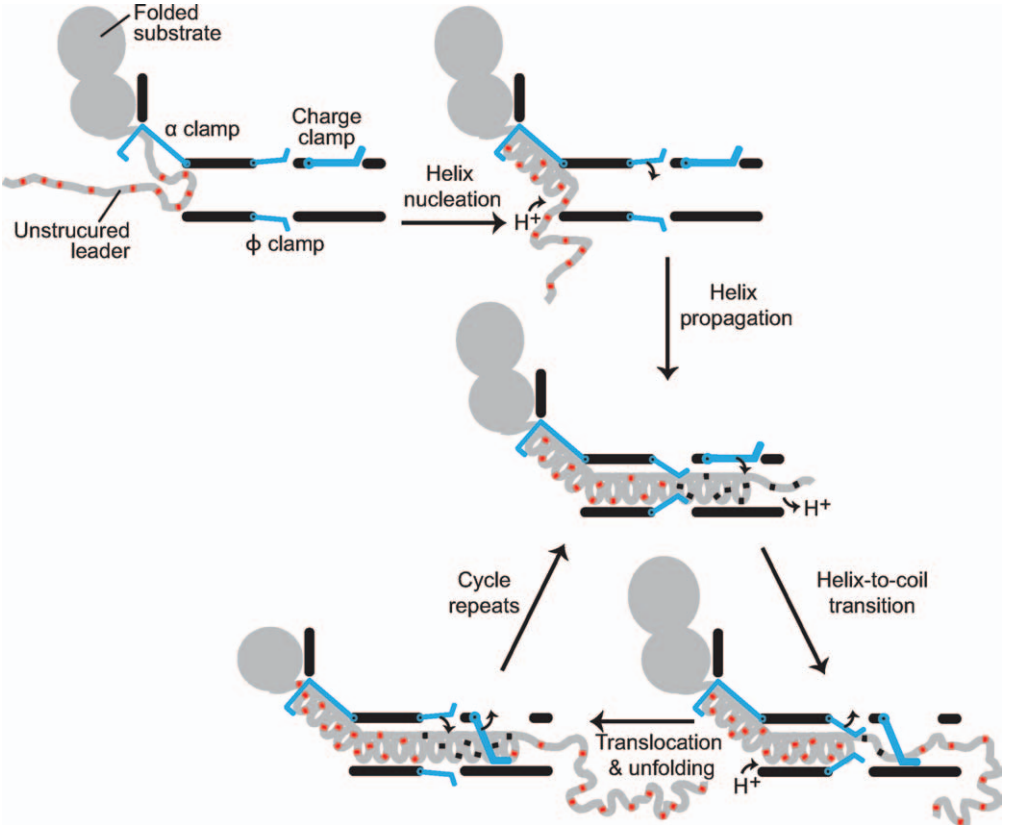

Figure 6. Translocation by a proton-driven engine. Folded substrate and unstructured leader sequence (gray) bind and dock to the PA channel. The α clamp nucleates and subsequently propagates helix formation. The ϕ clamp engages the compact translocating chain; deprotonated acidic residues (red) are then protonated (black). An increase in $T\Delta S_{config}$ outside the channel favors the transition of helix to unstructured random coil; acidic residues deprotonate in the higher pH of the cytosol. The charge clamp engages, permitting the passage of protonated acidic residues while preventing the retrotranslocation of deprotonated ones. Ungating of the ϕ clamp allows the chain to translocate, while the α clamp continues to stabilize and template unfolded polypeptide into helix. The cycle repeats until the substrate is fully unfolded and translocated.

further strengthened by the reduction in negative charge of the substrate.

- *Step 3.* While the substrate polypeptide is tightly engaged at the ϕ clamp, the amino-terminal end of the peptide eventually begins to extrude from the end of the channel, where conformational space of the chain is less restricted. Translocation is thus thermodynamically favorable in the direction out of the channel due to the gain in $T\Delta S_{config}$. Importantly, the peptide can bypass the anionic charge repulsion site in the channel, since the peptide is now protonated at its Asp and Glu sites.
- *Step 4.* The ΔpH at the ϕ clamp weakens as the substrate in the β barrel loses structure, solvent penetrates up the barrel, and H^+ dissipate out of the channel. The ϕ clamp switches to the *open* state, releasing bound peptide. Due to the charge selectivity of the channel, the peptide may only proceed through the channel until peptide and channel are no longer electrostatically compatible. At this point, translocation pauses until peptide recompresses into helix, the ϕ-clamp site can reset, and the deprotonated section of chain is protonated. The cycle will repeat in a fashion analogous to the thermodynamic cycles of a heat engine.

An entropic force generation mechanism

How much force may be generated during this proton engine's power stroke? In this mechanism, the power stroke is defined by the distance over which potential energy, stored in the form of compressed and ordered substrate polypeptide conformations, is released into relaxed and disordered conformations. Assuming an α-helical compressed state, which has threefold fewer degrees of freedom per residue than the fully random coil state, the mechanochemistry of this process is: $F = T\Delta S_{config}/d$, where d is the difference in length of peptide undergoing a α-helix-to-coil transition (2.2 Å per residue). F works out to ~20 pN—enough force to greatly accelerate protein unfolding reactions.[102,107-109] This calculation is an upper-limit. These forces are significant and higher than those estimated for BR models, where the substrate is a simple Brownian particle with only three translational degrees of freedom. The step size of the

anthrax toxin translocase has yet to be reported; however, the ~10-nm long β barrel likely places an order of magnitude limit on the power stroke length. Interestingly, the productive force generated over the range of the step as helix melts into random coil would not decrease over distance translocated. Conversely, the electrostatic force arising from the developing charge repulsion between the channel and peptide would decrease inversely as the square of the distance translocated. Here, we do not assume that the power stroke is largely dependent on the electrostatic repulsion between the substrate chain and the channel. Such an electrostatic force should not be ignored, although it would tend to occur over shorter distances.

The electrostatic repulsion may be considered the trigger that switches the translocase-substrate interaction between high-affinity and low-affinity modes, preventing unproductive motions. This electrostatic switch is akin to Maxwell's demon-operated trapdoor or any directionally biased ratchet. Conformational switching is generally what is observed for many ATPases and GTPases, and we expect switching to be a possible means by which both proton and ATP power sources are utilized. The available free energy dissipated by the pH gradient itself is more than adequate to supply the switch with the necessary power to drive the system and rectify the expansion direction of a more compacted α-helical peptide conformation to a more disordered state.

Acknowledgments

The authors thank Prof. Mark Fisher at the University of Kansas Medical Center for graciously providing an EM density map of the PA_7 channel. The authors also thank members of the Krantz lab and Prof. Ahmet Yildiz for helpful discussions.

References

1. Thoren KL, Krantz BA (2011) The unfolding story of anthrax toxin translocation. Mol Microbiol 80:588–595.
2. Matouschek A (2003) Protein unfolding--an important process in vivo? Curr Opin Struct Biol 13:98–109.
3. Prakash S, Matouschek A (2004) Protein unfolding in the cell. Trends Biochem Sci 29:593–600.
4. Wickner W, Schekman R (2005) Protein translocation across biological membranes. Science 310:1452–1456.
5. Sauer RT, Baker TA (2011) AAA+ proteases: ATP-fueled machines of protein destruction. Annu Rev Biochem 80:587–612.
6. Sauer RT, Bolon DN, Burton BM, Burton RE, Flynn JM, Grant RA, Hersch GL, Joshi SA, Kenniston JA, Levchenko I, Neher SB, Oakes ES, Siddiqui SM, Wah DA, Baker TA (2004) Sculpting the proteome with AAA(+) proteases and disassembly machines. Cell 119:9–18.
7. Gennerich A, Vale RD (2009) Walking the walk: how kinesin and dynein coordinate their steps. Curr Opin Cell Biol 21:59–67.
8. Maxwell JC (1871) Theory of heat. Mineola, New York: Dover Publications, Inc.
9. Thomson SW (1874) Kinetic theory of the dissipation of energy. Nature 9:441–444.
10. Sullivan MV (1946) Activated amusement device. U.S. Patent 2,402,463.
11. Carnot S (1824) Reflexions sur la puissance motrice du feu et sur les machines propres a developper cette puissance, Bachelier, Paris.
12. Smoluchowski M (1912) Experimentell nachweisbare, der Ublichen Thermodynamik widersprechende Molekularphenomene. Phys Zeitshur 13:1069–1079.
13. Feynman RP, Leighton RB, Sands M (1963) The Feynman lectures on physics. Reading, MA: Addison-Wesley, pp 46.41–46.49.
14. Smoluchowski M (1906) Zur kinetischen Theorie der Brownschen Molekularbewegung und der Suspensionen. Annalen der Physik 21:756–780.
15. Einstein A (1905) Über die von der molekularkinetischen Theorie der Wärme geforderte Bewegung von in ruhenden Flüssigkeiten suspendierten Teilchen. Annalen der Physik 17:549–560.
16. Langevin P (1908) Sur la théorie du mouvement brownien. C R Acad Sci (Paris) 146:530–533.
17. Lemons DS, Gythiel A (1997) Paul Langevin's 1908 paper "On the Theory of Brownian Motion" ["Sur la the'orie du mouvement brownien," C. R. Acad. Sci. (Paris) 146, 530–533 (1908)]. Am J Phys 65:1079–1081.
18. Tomkiewicz D, Nouwen N, Driessen AJ (2007) Pushing, pulling and trapping--modes of motor protein supported protein translocation. FEBS Lett 581:2820–2828.
19. Simon SM, Peskin CS, Oster GF (1992) What drives the translocation of proteins? Proc Natl Acad Sci USA 89:3770–3774.
20. Astumian RD (1997) Thermodynamics and kinetics of a Brownian motor. Science 276:917–922.
21. Krantz BA, Finkelstein A, Collier RJ (2006) Protein translocation through the anthrax toxin transmembrane pore is driven by a proton gradient. J Mol Biol 355:968–979.
22. Brown MJ, Thoren KL, Krantz BA (2011) Charge requirements for proton gradient-driven translocation of anthrax toxin. J Biol Chem 286:23189–23199.
23. Matlack KES, Misselwitz B, Plath K, Rapoport TA (1999) BiP Acts as a molecular ratchet during post-translational transport of prepro-alpha factor across the ER membrane. Cell 97:553–564.
24. Liebermeister W, Rapoport TA, Heinrich R (2001) Ratcheting in post-translational protein translocation: a mathematical model. J Mol Biol 305:643–656.
25. Glick BS (1995) Can Hsp70 proteins act as force-generating motors? Cell 80:11–14.
26. Bier M (2003) Processive motor protein as an overdamped brownian stepper. Phys Rev Lett 91:148104.
27. Horwich AL, Fenton WA (2009) Chaperonin-mediated protein folding: using a central cavity to kinetically assist polypeptide chain folding. Q Rev Biophys 42:83–116.
28. Merdanovic M, Clausen T, Kaiser M, Huber R, Ehrmann M (2011) Protein quality control in the bacterial periplasm. Annu Rev Microbiol 65:149–168.
29. Rapoport TA (2007) Protein translocation across the eukaryotic endoplasmic reticulum and bacterial plasma membranes. Nature 450:663–669.
30. Drazin R, Kandel J, Collier RJ (1971) Structure and activity of diphtheria toxin. II. Attack by trypsin at a specific site within the intact toxin molecule. J Biol Chem 246:1504–1510.
31. Barth H, Aktories K, Popoff MR, Stiles BG (2004) Binary bacterial toxins: biochemistry, biology, and applications of common Clostridium and Bacillus proteins. Microbiol Mol Biol Rev 68:373–402.

32. Falnes PO, Sandvig K (2000) Penetration of protein toxins into cells. Curr Opin Cell Biol 12:407–413.
33. Collier RJ (2009) Membrane translocation by anthrax toxin. Mol Aspects Med 30:413–422.
34. Young JA, Collier RJ (2007) Anthrax toxin: receptor binding, internalization, pore formation, and translocation. Annu Rev Biochem 76:243–265.
35. Feld GK, Kintzer AF, Tang,II, Thoren KL, Krantz BA (2012) Domain flexibility modulates the heterogeneous assembly mechanism of anthrax toxin protective antigen. J Mol Biol 415:159–174.
36. Pannifer AD, Wong TY, Schwarzenbacher R, Renatus M, Petosa C, Bienkowska J, Lacy DB, Collier RJ, Park S, Leppla SH, Hanna P, Liddington RC (2001) Crystal structure of the anthrax lethal factor. Nature 414:229–233.
37. Shen Y, Zhukovskaya NL, Guo Q, Florian J, Tang WJ (2005) Calcium-independent calmodulin binding and two-metal-ion catalytic mechanism of anthrax edema factor. EMBO J 24:929–941.
38. Feld GK, Thoren KL, Kintzer AF, Sterling HJ, Tang,II, Greenberg SG, Williams ER, Krantz BA (2010) Structural basis for the unfolding of anthrax lethal factor by protective antigen oligomers. Nature Struct Mol Biol 17:1383–1390.
39. Katayama H, Janowiak BE, Brzozowski M, Juryck J, Falke S, Gogol EP, Collier RJ, Fisher MT (2008) GroEL as a molecular scaffold for structural analysis of the anthrax toxin pore. Nature Struct Mol Biol 15: 754–760.
40. Kintzer AF, Thoren KL, Sterling HJ, Dong KC, Feld GK, Tang II, Zhang TT, Williams ER, Berger JM, Krantz BA (2009) The protective antigen component of anthrax toxin forms functional octameric complexes. J Mol Biol 392:614–629.
41. Mogridge J, Cunningham K, Collier RJ (2002) Stoichiometry of anthrax toxin complexes. Biochemistry 41: 1079–1082.
42. Lacy DB, Wigelsworth DJ, Melnyk RA, Harrison SC, Collier RJ (2004) Structure of heptameric protective antigen bound to an anthrax toxin receptor: a role for receptor in pH-dependent pore formation. Proc Natl Acad Sci USA 101:13147–13151.
43. Santelli E, Bankston LA, Leppla SH, Liddington RC (2004) Crystal structure of a complex between anthrax toxin and its host cell receptor. Nature 430: 905–908.
44. Lacy DB, Lin HC, Melnyk RA, Schueler-Furman O, Reither L, Cunningham K, Baker D, Collier RJ (2005) A model of anthrax toxin lethal factor bound to protective antigen. Proc Natl Acad Sci USA 102:16409–16414.
45. Miller CJ, Elliott JL, Collier RJ (1999) Anthrax protective antigen: prepore-to-pore conversion. Biochemistry 38:10432–10441.
46. Blaustein RO, Koehler TM, Collier RJ, Finkelstein A (1989) Anthrax toxin: channel-forming activity of protective antigen in planar phospholipid bilayers. Proc Natl Acad Sci USA 86:2209–2213.
47. Nguyen T (2004) Three-dimensional model of the pore form of anthrax protective antigen. Structure and biological implications. J Biomol Struct Dyn 22:253–265.
48. Krantz BA, Trivedi AD, Cunningham K, Christensen KA, Collier RJ (2004) Acid-induced unfolding of the amino-terminal domains of the lethal and edema factors of anthrax toxin. J Mol Biol 344:739–756.
49. Thoren KL, Worden EJ, Yassif JM, Krantz BA (2009) Lethal factor unfolding is the most force-dependent step of anthrax toxin translocation. Proc Natl Acad Sci USA 106:21555–21560.
50. Zhang S, Udho E, Wu Z, Collier RJ, Finkelstein A (2004) Protein translocation through anthrax toxin channels formed in planar lipid bilayers. Biophys J 87:3842–3849.
51. Basilio D, Kienker PK, Briggs SW, Finkelstein A (2011) A kinetic analysis of protein transport through the anthrax toxin channel. J Gen Physiol 137:521–531.
52. Krantz BA, Melnyk RA, Zhang S, Juris SJ, Lacy DB, Wu Z, Finkelstein A, Collier RJ (2005) A phenylalanine clamp catalyzes protein translocation through the anthrax toxin pore. Science 309:777–781.
53. Pentelute BL, Sharma,O., Collier,R.J. (2011) Chemical dissection of protein translocation through the anthrax toxin pore. Angew Chem Int Ed Engl 50:2294–2296.
54. Pentelute BL, Barker AP, Janowiak BE, Kent SB, Collier RJ (2010) A semisynthesis platform for investigating structure-function relationships in the N-terminal domain of the anthrax Lethal Factor. ACS Chem Biol 5:359–364.
55. Basilio D, Jennings-Antipov LD, Jakes KS, Finkelstein A (2011) Trapping a translocating protein within the anthrax toxin channel: implications for the secondary structure of permeating proteins. J Gen Physiol 137:343–356.
56. Basilio D, Juris SJ, Collier RJ, Finkelstein A (2009) Evidence for a proton-protein symport mechanism in the anthrax toxin channel. J Gen Physiol 133:307–314.
57. Janowiak BE, Fischer A, Collier RJ (2010) Effects of introducing a single charged residue into the phenylalanine clamp of multimeric anthrax protective antigen. J Biol Chem 285:8130–8137.
58. Fischer A, Holden MA, Pentelute BL, Collier RJ (2011) Ultrasensitive detection of protein translocated through toxin pores in droplet-interface bilayers. Proc Natl Acad Sci USA 108:16577–16581.
59. Blaustein RO, Lea EJ, Finkelstein A (1990) Voltage-dependent block of anthrax toxin channels in planar phospholipid bilayer membranes by symmetric tetraalkylammonium ions. Single-channel analysis. J Gen Physiol 96:921–942.
60. Harsman A, Bartsch P, Hemmis B, Kruger V, Wagner R (2011) Exploring protein import pores of cellular organelles at the single molecule level using the planar lipid bilayer technique. Eur J Cell Biol 90:721–730.
61. Grigoriev SM, Muro C, Dejean LM, Campo ML, Martinez-Caballero S, Kinnally KW (2004) Electrophysiological approaches to the study of protein translocation in mitochondria. Int Rev Cytol 238:227–274.
62. Henry JP, Juin P, Vallette F, Thieffry M (1996) Characterization and function of the mitochondrial outer membrane peptide-sensitive channel. J Bioenerg Biomembr 28:101–108.
63. Movileanu L, Schmittschmitt JP, Scholtz JM, Bayley H (2005) Interactions of peptides with a protein pore. Biophys J 89:1030–1045.
64. Mahendran KR, Romero-Ruiz M, Schlosinger A, Winterhalter M, Nussberger S (2012) Protein translocation through Tom40: kinetics of peptide release. Biophys J 102:39–47.
65. Senzel L, Huynh PD, Jakes KS, Collier RJ, Finkelstein A (1998) The diphtheria toxin channel-forming T domain translocates its own NH2-terminal region across planar bilayers. J Gen Physiol 112:317–324.
66. Montal M (2009) Translocation of botulinum neurotoxin light chain protease by the heavy chain protein-conducting channel. Toxicon 54:565–569.
67. Hoch DH, Romero-Mira M, Ehrlich BE, Finkelstein A, DasGupta BR, Simpson LL (1985) Channels formed by botulinum, tetanus, and diphtheria toxins in

planar lipid bilayers: relevance to translocation of proteins across membranes. Proc Natl Acad Sci USA 82: 1692–1696.
68. Petosa C, Collier RJ, Klimpel KR, Leppla SH, Liddington RC (1997) Crystal structure of the anthrax toxin protective antigen. Nature 385:833–838.
69. Katayama H, Wang J, Tama F, Chollet L, Gogol EP, Collier RJ, Fisher MT (2010) Three-dimensional structure of the anthrax toxin pore inserted into lipid nanodiscs and lipid vesicles. Proc Natl Acad Sci USA 107:3453–3457.
70. Drum CL, Yan SZ, Bard J, Shen YQ, Lu D, Soelaiman S, Grabarek Z, Bohm A, Tang WJ (2002) Structural basis for the activation of anthrax adenylyl cyclase exotoxin by calmodulin. Nature 415:396–402.
71. Jennings-Antipov LD, Song L, Collier RJ (2011) Interactions of anthrax lethal factor with protective antigen defined by site-directed spin labeling. Proc Natl Acad Sci USA 108:1868–1873.
72. Molloy SS, Bresnahan PA, Leppla SH, Klimpel KR, Thomas G (1992) Human furin is a calcium-dependent serine endoprotease that recognizes the sequence Arg-X-X-Arg and efficiently cleaves anthrax toxin protective antigen. J Biol Chem 267:16396–16402.
73. Klimpel KR, Molloy SS, Thomas G, Leppla SH (1992) Anthrax toxin protective antigen is activated by a cell surface protease with the sequence specificity and catalytic properties of furin. Proc Natl Acad Sci USA 89: 10277–10281.
74. Milne JC, Furlong D, Hanna PC, Wall JS, Collier RJ (1994) Anthrax protective antigen forms oligomers during intoxication of mammalian cells. J Biol Chem 269:20607–20612.
75. Kintzer AF, Sterling HJ, Tang II, Abdul-Gader A, Miles AJ, Wallace BA, Williams ER, Krantz BA (2010) Role of the protective antigen octamer in the molecular mechanism of anthrax lethal toxin stabilization in plasma. J Mol Biol 399:741–758.
76. Cunningham K, Lacy DB, Mogridge J, Collier RJ (2002) Mapping the lethal factor and edema factor binding sites on oligomeric anthrax protective antigen. Proc Natl Acad Sci USA 99:7049–7053.
77. Chauhan V, Bhatnagar R (2002) Identification of amino acid residues of anthrax protective antigen involved in binding with lethal factor. Infect Immun 70:4477–4484.
78. Lacy DB, Mourez M, Fouassier A, Collier RJ (2002) Mapping the anthrax protective antigen binding site on the lethal and edema factors. J Biol Chem 277: 3006–3010.
79. Mourez M, Yan M, Lacy DB, Dillon L, Bentsen L, Marpoe A, Maurin C, Hotze E, Wigelsworth D, Pimental RA, Ballard JD, Collier RJ, Tweten RK (2003) Mapping dominant-negative mutations of anthrax protective antigen by scanning mutagenesis. Proc Natl Acad Sci USA 100:13803–13808.
80. Melnyk RA, Hewitt KM, Lacy DB, Lin HC, Gessner CR, Li S, Woods VL, Jr, Collier RJ (2006) Structural determinants for the binding of anthrax lethal factor to oligomeric protective antigen. J Biol Chem 281: 1630–1635.
81. Schueler-Furman O, Wang C, Baker D (2005) Progress in protein-protein docking: atomic resolution predictions in the CAPRI experiment using RosettaDock with an improved treatment of side-chain flexibility. Proteins 60:187–194.
82. Bradley KA, Mogridge J, Mourez M, Collier RJ, Young JA (2001) Identification of the cellular receptor for anthrax toxin. Nature 414:225–229.
83. Scobie HM, Rainey GJA, Bradley KA, Young JA (2003) Human capillary morphogenesis protein 2 functions as an anthrax toxin receptor. Proc Natl Acad Sci USA 100:5170–5174.
84. Koehler TM, Collier RJ (1991) Anthrax toxin protective antigen: low-pH-induced hydrophobicity and channel formation in liposomes. Mol Microbiol 5:1501–1506.
85. Qa'dan M, Christensen KA, Zhang L, Roberts TM, Collier RJ (2005) Membrane insertion by anthrax protective antigen in cultured cells. Mol Cell Biol 25: 5492–5498.
86. Friedlander AM (1986) Macrophages are sensitive to anthrax lethal toxin through an acid-dependent process. J Biol Chem 261:7123–7126.
87. Zhang S, Finkelstein A, Collier RJ (2004) Evidence that translocation of anthrax toxin's lethal factor is initiated by entry of its N terminus into the protective antigen channel. Proc Natl Acad Sci USA 101: 16756–16761.
88. Blanke SR, Milne JC, Benson EL, Collier RJ (1996) Fused polycationic peptide mediates delivery of diphtheria toxin A chain to the cytosol in the presence of anthrax protective antigen. Proc Natl Acad Sci USA 93:8437–8442.
89. Finkelstein A (2009) Proton-coupled protein transport through the anthrax toxin channel. Philos Trans R Soc Lond B Biol Sci 364:209–215.
90. Kintzer AF, Sterling HJ, Tang II, Williams ER, Krantz BA (2010) Anthrax toxin receptor drives protective antigen oligomerization and stabilizes the heptameric and octameric oligomer by a similar mechanism. PLoS ONE 5:e13888.
91. Nassi S, Collier RJ, Finkelstein A (2002) PA_{63} channel of anthrax toxin: an extended β-barrel. Biochemistry 41:1445–1450.
92. Benson EL, Huynh PD, Finkelstein A, Collier RJ (1998) Identification of residues lining the anthrax protective antigen channel. Biochemistry 37:3941–3948.
93. Meador WE, Means AR, Quiocho FA (1993) Modulation of calmodulin plasticity in molecular recognition on the basis of x-ray structures. Science 262:1718–1721.
94. Zimm GH, Bragg JK (1959) Theory of the phase transition between helix and random coil in polypeptide chains. J Chem Phys 31:526–535.
95. Meador WE, Means AR, Quiocho FA (1992) Target enzyme recognition by calmodulin: 2.4 A structure of a calmodulin-peptide complex. Science 257:1251–1255.
96. Martin A, Baker TA, Sauer RT (2008) Pore loops of the AAA+ ClpX machine grip substrates to drive translocation and unfolding. Nat Struct Mol Biol 15: 1147–1151.
97. Kauzmann W (1959) Some factors in the interpretation of protein denaturation. Adv Protein Chem 14:1–64.
98. Tanford C (1968) Protein denaturation. Adv Protein Chem 23:121–282.
99. Dill KA, Fiebig K, M., Chan HS (1993) Cooperativity in protein-folding kinetics. Proc Natl Acad Sci USA 90:1942–1946.
100. Melnyk RA, Collier RJ (2006) A loop network within the anthrax toxin pore positions the phenylalanine clamp in an active conformation. Proc Natl Acad Sci USA 103:9802–9807.
101. Bann JG (2012) Anthrax toxin protective antigen-Insights into molecular switching from prepore to pore. Protein Sci 21:1–12.
102. Brockwell DJ, Paci E, Zinober RC, Beddard GS, Olmsted PD, Smith DA, Perham RN, Radford SE (2003) Pulling geometry defines the mechanical resistance of a beta-sheet protein. Nat Struct Biol 10:731–737.

103. Burton RE, Siddiqui SM, Kim YI, Baker TA, Sauer RT (2001) Effects of protein stability and structure on substrate processing by the ClpXP unfolding and degradation machine. EMBO J 20:3092–3100.
104. Huang S, Ratliff KS, Schwartz MP, Spenner JM, Matouschek A (1999) Mitochondria unfold precursor proteins by unraveling them from their N-termini. Nat Struct Biol 6:1132–1138.
105. Kenniston JA, Baker TA, Fernandez JM, Sauer RT (2003) Linkage between ATP consumption and mechanical unfolding during the protein processing reactions of an AAA+ degradation machine. Cell 114:511–520.
106. Krantz BA, Mayne L, Rumbley J, Englander SW, Sosnick TR (2002) Fast and slow intermediate accumulation and the initial barrier mechanism in protein folding. J Mol Biol 324:359–371.
107. Cecconi C, Shank EA, Bustamante C, Marqusee S (2005) Direct observation of the three-state folding of a single protein molecule. Science 309:2057–2060.
108. Borgia A, Williams PM, Clarke J (2008) Single-molecule studies of protein folding. Annu Rev Biochem 77: 101–125.
109. Crampton N, Brockwell DJ (2010) Unravelling the design principles for single protein mechanical strength. Curr Opin Struct Biol 20:508–517.
110. Maillard RA, Chistol G, Sen M, Righini M, Tan J, Kaiser CM, Hodges C, Martin A, Bustamante C (2011) ClpX(P) generates mechanical force to unfold and translocate its protein substrates. Cell 145:459–469.
111. Tian L, Holmgren RA, Matouschek A (2005) A conserved processing mechanism regulates the activity of transcription factors Cubitus interruptus and NF-kappaB. Nat Struct Mol Biol 12:1045–1053.
112. Page MI, Jencks WP (1971) Entropic contributions to rate accelerations in enzymic and intramolecular reactions and the chelate effect. Proc Natl Acad Sci USA 68:1678–1683.
113. Wesche J, Elliott JL, Falnes PO, Olsnes S, Collier RJ (1998) Characterization of membrane translocation by anthrax protective antigen. Biochemistry 37:15737–15746.
114. Milne JC, Blanke SR, Hanna PC, Collier RJ (1995) Protective antigen-binding domain of anthrax lethal factor mediates translocation of a heterologous protein fused to its amino- or carboxy-terminus. Mol Microbiol 15:661–666.
115. Dill KA (1990) Dominant forces in protein folding. Biochemistry 29:7133–7155.
116. Zhou H, Zhou Y (2002) Stability scale and atomic solvation parameters extracted from 1023 mutation experiments. Proteins 49:483–492.
117. Kenniston JA, Burton RE, Siddiqui SM, Baker TA, Sauer RT (2004) Effects of local protein stability and the geometric position of the substrate degradation tag on the efficiency of ClpXP denaturation and degradation. J Struct Biol 146:130–140.
118. Ashcroft F, Gadsby D, Miller C (2009) Introduction. The blurred boundary between channels and transporters. Philos Trans R Soc Lond B Biol Sci 364: 145–147.
119. Oomen CJ, Van Ulsen P, Van Gelder P, Feijen M, Tommassen J, Gros P (2004) Structure of the translocator domain of a bacterial autotransporter. EMBO J 23: 1257–1266.
120. Meng G, Surana,N.K., St. Geme,J.W. 3rd, Waksman,G. (2006) Structure of the outer membrane translocator domain of the *Haemophilus influenzae* Hia trimeric autotransporter. EMBO J 25:2297–2304.
121. Ramachandran GN, Sasisekharan V (1968) Conformation of polypeptides and proteins. Adv Protein Chem 23:283–438.